An Analysis of Fully Developed Laminar Flow in an Eccentric Annulus

WILLIAM T. SNYDER and GERALD A. GOLDSTEIN

University of Tennessee Space Institute, Tullahoma, Tennessee

An analysis is presented of fully developed laminar flow in an eccentric annulus. An exact solution for the velocity distribution is presented. From this solution may be obtained expressions for local shear stress on the inner and outer surfaces of the annulus, friction factors based on the inner and outer surfaces, and the overall friction factor. Curves of these data are presented covering a range of eccentricity values and radius ratio values.

In recent years, a considerable interest has developed in the problems of flow and heat transfer in annuli, both concentric and eccentric. In addition to its inherent usefulness as a flow geometry, flow in an annulus has proved useful as a model for longitudinal flow in a tube bundle (*5*). The interest in the eccentric annulus arises because of the problem of tube misalignment which frequently occurs in a close-packed tubular heat exchanger. A considerable amount of work has been done on the problem of turbulent flow in an eccentric annulus (*4*), but to the authors' knowledge no results have been reported for the laminar flow friction factors in an eccentric annulus. The present investigation attempts to fill this gap in the knowledge of annulus flows.

In a recent paper (*1*), the problem of slug flow heat transfer in an eccentric annulus was considered. The governing equation for both slug flow heat transfer and fully developed laminar flow in an eccentric annulus is Poisson's equation with a constant nonhomogeneous term. Thus the governing equation for the present investigation is the same as that employed in reference *1* with different boundary conditions. The basic mathematical technique applicable to both problems is the bipolar transformation which maps the concentric annulus cross section in the physical plane into a rectangle in the complex plane.

An analysis of the laminar flow problem by Heyda (*2*) was recently called to the authors' attention. Heyda's main interest was establishing the locus of maximum velocity for fully developed laminar flow in an eccentric annulus. The assumption was then made that the locus of maximum velocity would be the same for both laminar and turbulent flow, an assumption which has been recently verified over a limited range of radius ratios by Wolffe and Clump (*3*). The expression for the shear stress was not obtained by Heyda, and no numerical results were presented.

In the present analysis, a solution is obtained for the fully developed laminar flow velocity distribution in an eccentric annulus. From this solution, expressions are obtained for the variation of local shear stress around the inner and outer surfaces of the annulus. Friction factors are defined for each surface as well as a total friction factor based on the total shear at both surfaces. Numerical results are presented covering a range of eccentricities and radius ratios.

Gerald A. Goldstein is at the State University of New York at Stony Brook, Stony Brook, New York.

THE ANALYSIS

The geometry considered in the present analysis is shown in Figure 1. The equation of motion for fully developed laminar flow may be written as

$$\frac{1}{\mu}\frac{dP}{dz} = \frac{\partial^2 u}{\partial x^2} + \frac{\partial^2 u}{\partial y^2} \qquad (1)$$

where the pressure gradient is constant because of the assumption of fully developed flow. The viscosity will be assumed constant. The boundary conditions are the nonslip conditions expressed by $u = 0$ at the inner and outer surfaces.

Because of the asymmetry of the geometry, cylindrical coordinates cannot be used, and bipolar coordinates (*6*) must be used. Equation (1) is transformed to the bipolar coordinate system and a solution obtained in this system. The details of the transformation and solution technique are similar to those employed in reference *1* and in a paper by El-Saden (*7*) in which the problem of heat conduction in an eccentrically hollow cylinder was solved. The bipolar coordinates (η, ξ) are defined by the transformation

$$x + iy = ic \cot\left(\frac{\xi + i\eta}{2}\right) \qquad (2)$$

where c is a constant and $i = \sqrt{-1}$. Equating real and imaginary parts of Equation (2) one gets relations between the physical and bipolar coordinates in the form

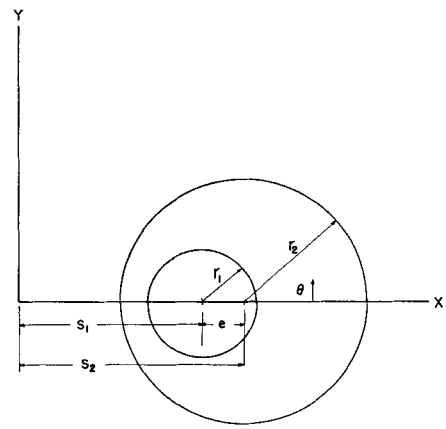

Fig. 1. Eccentric annulus geometry.

$$x = \frac{c \sinh \eta}{\cosh \eta - \cos \xi} \tag{3a}$$

$$y = \frac{c \sin \xi}{\cosh \eta - \cos \xi} \tag{3b}$$

$$e^{2\eta} = \frac{y^2 + (x+c)^2}{y^2 + (x-c)^2} \tag{3c}$$

$$\tan \xi = \frac{2yc}{x^2 + y^2 - c^2} \tag{3d}$$

$$y^2 + (x - c \coth \eta)^2 = \frac{c^2}{\sinh^2 \eta} \tag{3e}$$

Equation (3e) shows that lines of constant η represent circles in the physical plane with center at (c coth η, 0) and radius $c/\sinh \eta$. The inner and outer surfaces of the annulus are thus represented by lines of constant η which will be designated as α and β, respectively. With this notation, it may be shown from geometrical considerations that the constants c, α, and β are given by the expressions

$$c = r_1 \sinh \alpha = r_2 \sinh \beta \tag{4a}$$

$$\cosh \alpha = \frac{1}{\gamma} \frac{\gamma(1+\phi^2) + (1-\phi^2)}{2\phi} \tag{4b}$$

$$\cosh \beta = \frac{\gamma(1-\phi^2) + (1+\phi^2)}{2\phi} \tag{4c}$$

where

$$\gamma = \frac{r_1}{r_2} \tag{4d}$$

$$\phi = \frac{e}{r_2 - r_1} \tag{4e}$$

The detailed transformation of the Laplacian operator is contained in reference 9.

Transforming Equation (1) into bipolar coordinates one gets

$$\frac{\partial^2 v}{\partial \xi^2} + \frac{\partial^2 v}{\partial \eta^2} = -\frac{1}{(\cosh \eta - \cos \xi)^2} \tag{5a}$$

where

$$v = -\frac{u}{\frac{c^2}{\mu}\frac{dP}{dz}} \tag{5b}$$

is the dimensionless velocity. The general solution to Equation (5a) is given in reference 7. Applying the boundary conditions $v(\eta = \alpha) = 0 = v(\eta = \beta)$ one obtains the general solution in the form

$$v = F + E\eta - \frac{ctnh\, \eta}{2} + \sum_{n=1}^{\infty} \{A_n e^{n\eta} + (B_n - ctnh\, \eta)\, e^{-n\eta}\} \cos n\xi \tag{6a}$$

where

$$F = \frac{\alpha\, ctnh\, \beta - \beta\, ctnh\, \alpha}{2(\alpha - \beta)} \tag{6b}$$

$$E = \frac{ctnh\alpha - ctnh\beta}{2(\alpha - \beta)} \tag{6c}$$

$$A_n = \frac{ctnh\alpha - ctnh\beta}{e^{2n\alpha} - e^{2n\beta}} \tag{6d}$$

$$B_n = \frac{e^{2n\alpha}\, ctnh\beta - e^{2n\beta}\, ctnh\alpha}{e^{2n\alpha} - e^{2n\beta}} \tag{6e}$$

For a given geometry, γ and ϕ, defined by Equations (4d) and (4e), would be specified. These values then determine α and β, given by Equations (4b) and (4c), respectively. With α and β determined, the constants appearing in Equation (6a), defined by Equations (6b) to (6e), are then fixed.

LOCAL WALL SHEAR STRESS

The local wall stress may be determined by evaluating the velocity gradient at the wall. Thus

$$\tau_{wall} = \pm \mu \left.\frac{\partial u}{\partial r}\right)_{wall} \tag{7}$$

where r is the radial coordinate measured from the center of the circle on which τ_{wall} is being calculated. The algebraic sign is chosen to make τ_{wall} a positive quantity. Since $\left.\frac{\partial u}{\partial r}\right)_{wall} > 0$ on the inner wall and $\left.\frac{\partial u}{\partial r}\right)_{wall} < 0$ on the outer wall, choosing the plus sign for the inner wall and the minus sign for the outer wall will give positive values for τ_{wall} in both cases.

The velocity gradient in the r direction must be expressed in terms of the (ξ, η) bipolar coordinates. This transformation involves a straightforward application of the chain rule of partial differentiation. The details are presented in the Appendix, and the final results may be written as

$$\tau_{\substack{inner\\wall}} = \tau_1 = \frac{\mu(1 - \cosh \alpha \cos \xi)}{r_1 \sinh \alpha \cos \theta} \left.\frac{\partial u}{\partial \eta}\right)_{\eta=\alpha} \tag{8a}$$

$$\tau_{\substack{outer\\wall}} = \tau_2 = \frac{-\mu(1 - \cosh\beta \cos\xi)}{r_2 \sinh \beta \cos \theta} \left.\frac{\partial u}{\partial \eta}\right)_{\eta=\beta} \tag{8b}$$

where θ and ξ are related along the walls by the expressions

$$\tan \theta)_{\substack{inner\\wall}} = \frac{\sinh \alpha \sin \xi}{\cosh\alpha \cos \xi - 1} \tag{9a}$$

$$\tan \theta)_{\substack{outer\\wall}} = \frac{\sinh \beta \sin \xi}{\cosh \beta \cos \xi - 1} \tag{9b}$$

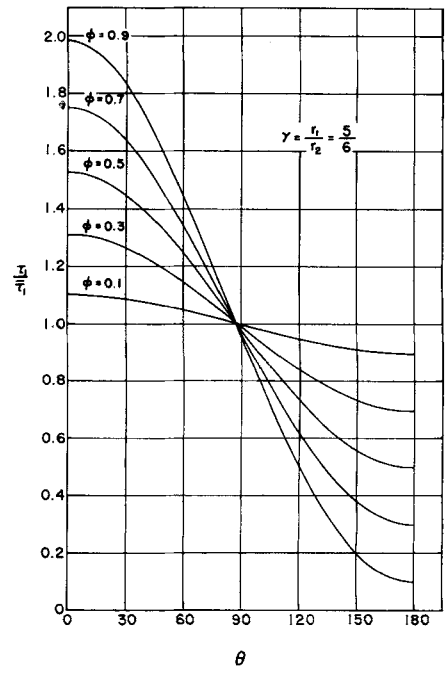

Fig. 2. Local shear stress on inner wall for $\gamma = 5/6$.

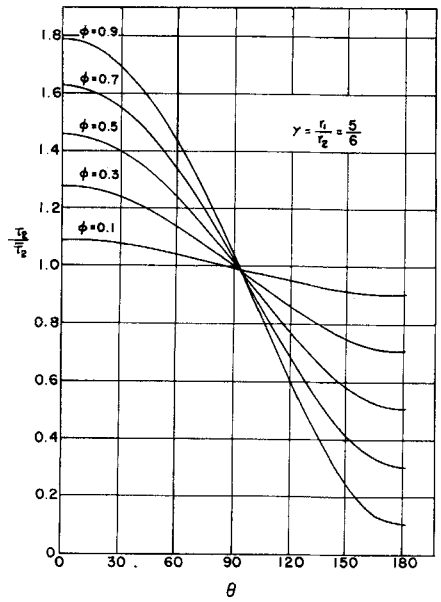

Fig. 3. Local shear stress on outer wall for $\gamma = 5/6$.

The average values of the wall shear stresses are given by

$$\tau_{1)\,avg} = \bar{\tau}_1 = \frac{1}{\pi}\int_o^\pi \tau_1\, d\theta \qquad (10a)$$

$$\tau_{2)\,avg} = \bar{\tau}_2 = \frac{1}{\pi}\int_o^\pi \tau_2\, d\theta \qquad (10b)$$

where the integration is performed only over the range $0 \leq \theta \leq \pi$ because of symmetry about the x axis. From Equations (8a) to (10b), values of $\tau_1/\bar{\tau}_1$ and $\tau_2/\bar{\tau}_2$ may be calculated which give the variation of local shear stress around the walls in dimensionless form. Equations (10a) and (10b) were evaluated numerically on an IBM-1620 computer.

INNER AND OUTER WALL FRICTION FACTORS

A friction factor may be defined relative to both the inner wall and outer wall average shear stresses by the relations

$$f_1 = \frac{\bar{\tau}_1}{\frac{\rho\,\bar{u}^2}{2}} \qquad (11a)$$

$$f_2 = \frac{\bar{\tau}_2}{\frac{\rho\,\bar{u}^2}{2}} \qquad (11b)$$

where $\bar{u}$ is the mean velocity defined as

$$\bar{u} = \frac{1}{\pi(r_2^2 - r_1^2)} \int\int u\, dA \qquad (12)$$

The differential element of area $dA = dx\,dy$ may be shown (*1*) to be related to the (ξ, η) coordinates through the expression

$$dA = dxdy = \frac{c^2\, d\xi\, d\eta}{(\cosh\eta - \cos\xi)^2} \qquad (13)$$

Equation (12) may then be rewritten as

$$\bar{u} = \frac{c^2}{\pi(r_2^2 - r_1^2)} \int_\alpha^\beta \int_o^{2\pi} \frac{u}{(\cosh\eta - \cos\xi)^2}\, d\xi\, d\eta =$$

$$\frac{-2c^4}{\pi\mu(r_2^2 - r_1^2)}\, I\, \frac{dP}{dz} \qquad (14a)$$

where

$$I = \int_\alpha^\beta \int_o^\pi \frac{v}{(\cosh\eta - \cos\xi)^2}\, d\xi\, d\eta \qquad (14b)$$

The overall force balance equation for the annulus may be written

$$2\pi(r_1\bar{\tau}_1 + r_2\bar{\tau}_2) = -\pi(r_2^2 - r_1^2)\frac{dP}{dz} \qquad (15a)$$

$$2r_1\bar{\tau}_1\left(1 + \frac{r_2}{r_1}\frac{\bar{\tau}_2}{\bar{\tau}_1}\right) = -(r_2^2 - r_1^2)\frac{dP}{dz} \qquad (15b)$$

$$2r_2\bar{\tau}_2\left(1 + \frac{r_1}{r_2}\frac{\bar{\tau}_1}{\bar{\tau}_2}\right) = -(r_2^2 - r_1^2)\frac{dP}{dz} \qquad (15c)$$

Combining Equations (11a), (11b), (14a), (15b), (15c) and introducing the Reynolds number defined as

$$N_{Re} = \frac{2\rho\,\bar{u}}{\mu}(r_2 - r_1) \qquad (16)$$

one gets

$$f_1 N_{Re} = \frac{\pi\left\{\left(\frac{r_2}{r_1}\right)^2 - 1\right\}^2 \left\{\frac{r_2}{r_1} - 1\right\}}{I\,\sinh^4\alpha\left\{1 + \frac{r_2}{r_1}\frac{\bar{\tau}_2}{\bar{\tau}_1}\right\}} \qquad (17a)$$

$$f_2 N_{Re} = \frac{\pi\left\{1 - \left(\frac{r_1}{r_2}\right)^2\right\}^2 \left\{1 - \frac{r_1}{r_2}\right\}}{I\,\sinh^4\beta\left\{1 + \frac{r_1}{r_2}\frac{\bar{\tau}_1}{\bar{\tau}_2}\right\}} \qquad (17b)$$

TOTAL FRICTION FACTOR

In reference 8, the average friction factor for the concentric annulus is defined as

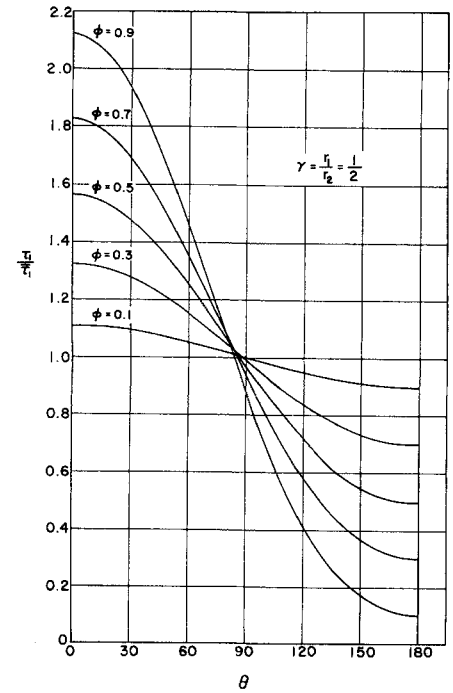

Fig. 4. Local shear stress on inner wall for $\gamma = \frac{1}{2}$.

$$f = \frac{-(r_2 - r_1)}{\bar{\rho}\bar{u}^2} \frac{dP}{dz} \qquad (18)$$

This same definition will be used for the average friction factor for the eccentric annulus. The pressure gradient may be related to f_1 and f_2 by an overall force balance

$$2\pi(r_1\bar{\tau}_1 + r_2\bar{\tau}_2) = -\pi(r_2^2 - r_1^2)\frac{dP}{dz} \qquad (19a)$$

or

$$\rho\bar{u}^2(r_1 f_1 + r_2 f_2) = -(r_2^2 - r_1^2)\frac{dP}{dz} \qquad (19b)$$

Combining Equations (18) and (19b) one obtains

$$fN_{Re} = \frac{\gamma f_1 N_{Re} + f_2 N_{Re}}{1 + \gamma} \qquad (20a)$$

where

$$\gamma = \frac{r_1}{r_2} \qquad (20b)$$

The use of the values of $f_1 N_{Re}$ and $f_2 N_{Re}$ calculated from Equations (17a) and (17b) in Equation (20a) determines the average friction factor-Reynolds number product.

NUMERICAL RESULTS

Numerical results for a range of radius ratios and eccentricities are shown in Figures 2 through 8. The distribution of local shear stress on the inner and outer surfaces is shown in Figures 2 through 5. The data are presented with the ratio of local to average wall stress plotted against angular position with eccentricity as parameter. As one would expect, the wall stress is largest in the region of smallest separation between the surfaces, corresponding to $\theta = 0$. It is interesting to note that the local wall stress may vary by as much as a factor of 20 over the range of eccentricities and radius ratios considered.

The friction factors for the inner and outer surfaces, defined by Equations (17a) and (17b), are shown in Figures 6 and 7 for two radius ratios. The friction factor for the outer wall is less than the corresponding quantity for the inner wall, the difference between the two quantities decreasing with increasing eccentricity. Also the difference between inner and outer wall friction factors appears to decrease as the ratio of inner tube diameter to outer tube diameter increases. This trend appears to be valid for all values of eccentricity.

The final data to be presented, shown in Figure 8, give the variation of total friction factor, defined by Equation (18), with eccentricity for fixed radius ratio. Two values of radius ratio, namely $\gamma = 1/2$ and $\gamma = 5/6$, are shown. As seen in Figure 8, the total friction factor is only slightly sensitive to radius ratio over the range covered but changes significantly with eccentricity. There is a change by a factor of approximately 2 over the range of eccentricity from 0.1 to 0.9.

NOTES ADDED IN REVIEW

One of the referees called to the authors' attention the work of Redberger and Charles (*10*). These authors presented a numerical solution, starting with Equation (5a)

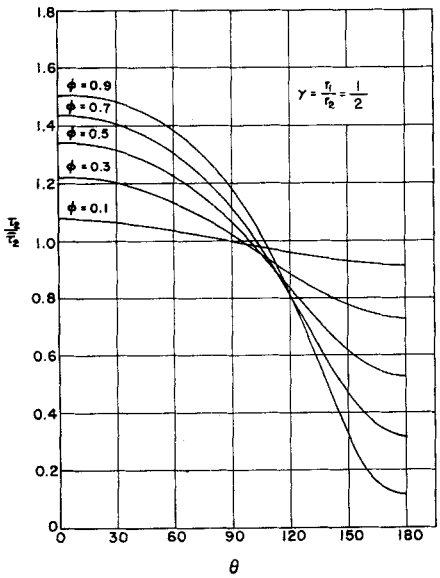

Fig. 5. Local shear stress on outer wall for $\gamma = 1/2$.

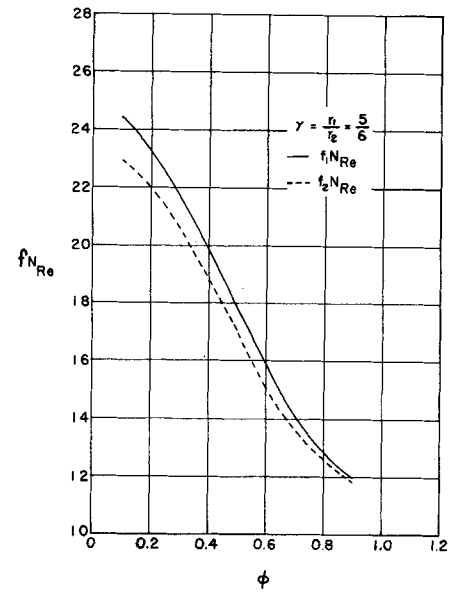

Fig. 6. Inner and outer wall friction factors for $\gamma = 5/6$.

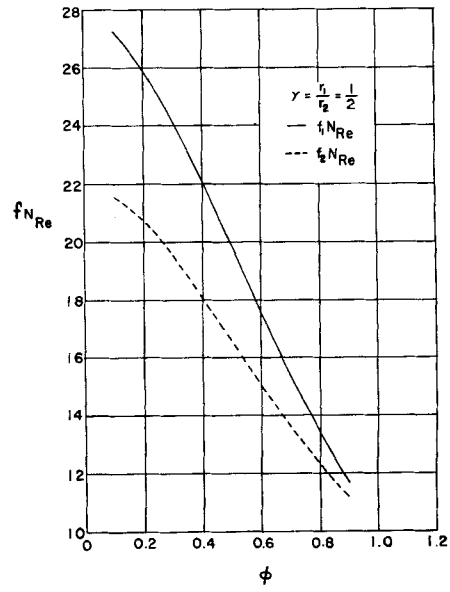

Fig. 7. Inner and outer wall friction factors for $\gamma = 1/2$.

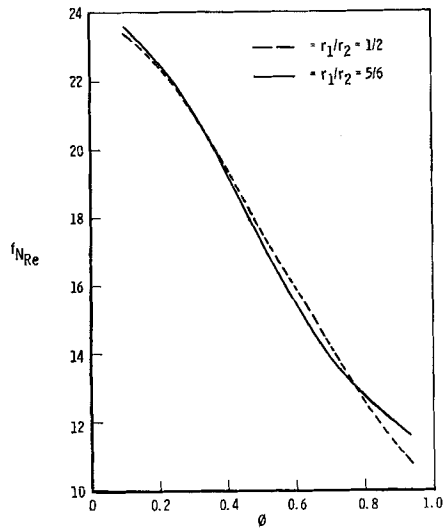

Fig. 8. Total friction factor for $\gamma = 1/2$ and $\gamma = 5/6$.

of the present paper written in finite difference form, of the ratio of mass flow rate between eccentric cylinders to the mass flow rate between concentric cylinders of the same diameter ratio. The local shear stress distribution on the surfaces was not presented.

It was also pointed out during the review that a body force could be included in the present results. If f_z is the component of body force in the direction of motion, Equation (1) becomes

$$-\frac{1}{\mu}f_z + \frac{1}{\mu}\frac{dP}{dz} = \frac{\partial^2 u}{\partial x^2} + \frac{\partial^2 u}{\partial y^2}$$

When one redefines the dimensionless velocity of Equation (5*b*) as

$$v = -\frac{u}{\frac{c^2}{\mu}\left(\frac{dP}{dz} - f_z\right)}$$

the results of the present analysis are valid for the case of a constant body force.

NOTATION

A_n, B_n, E, F = constants defined by Equation (6)
c = constant defined by Equation (4*a*)
e = eccentricity = $(r_2 - r_1)$
f_1, f_2, f = friction factors defined by Equations (11) and (18)
I = integral defined by Equation (14*b*)
P = pressure
r_1, r_2 = inner and outer radii, respectively
N_{Re} = Reynolds number defined by Equation (16)
u = velocity
$\bar{u}$ = average velocity
v = dimensionless velocity defined by Equation (5*b*)
x, y, z = space coordinates defined in Figure 1.

Greek Letters

α, β = constants defined by Equations (4*b*) and (4*c*)
γ = radius ratio = r_1/r_2
η, ξ = bipolar coordinates defined by Equations (3*c*) and (3*d*)
ϕ = eccentricity ratio = $e/r_2 - r_1$
τ_1, τ_2 = inner and outer wall local shear stresses
$\bar{\tau}_1$, $\bar{\tau}_2$ = inner and outer wall average shear stresses
μ = viscosity

LITERATURE CITED

1. Snyder, William T., *A.I.Ch.E. Journal*, **9**, No. 4, 503 (1963).
2. Heyda. J. F., General Electric Co. Report, APEX-391 (1958).
3. Wolffe, R. A., and C. W. Clump, *A.I.Ch.E. Journal*, **9**, No. 3, 424 (1963).
4. Rothfus, R. R., J. E. Walker, and G. A. Whan, *ibid.*, **4**, No. 2, 240 (1958).
5. Dwyer, O. E., and P. S. Tu, *Chem. Eng. Progr.*, **56**, No. 30, 183 (1960).
6. Batemann, Harry, "Partial Differential Equations of Mathematical Physics," p. 260, Dover Publications, New York (1944).
7. El-Saden, M. R., *J. Heat Transfer*, **83**, No. 4, 510 (1961).
8. Knudsen, J. G., and D. L. Katz, "Fluid Dynamics and Heat Transfer," p. 91, McGraw-Hill, New York (1958).
9. Moon, P. H., and D. E. Spencer, "Field Theory for Engineers," Van Nostrand, New York (1961).
10. Redberger, P. J., and M. E. Charles, *Can. J. Chem. Eng.*, 148, August (1962).

APPENDIX

Derivation of Wall Shear Stress Expression

The expression for the local wall shear stress is

$$\tau_{wall} = \pm \mu \left(\frac{\partial u}{\partial r}\right)_{wall} \tag{A1}$$

where r is the radial coordinate measured from the center of the circle on which τ_{wall} is being calculated. The velocity gradient at the wall can be evaluated from the chain rule as

$$\left(\frac{\partial u}{\partial r}\right)_{wall} = \left\{\left(\frac{\partial u}{\partial x}\right)_y \left(\frac{\partial x}{\partial r}\right)_\theta + \left(\frac{\partial u}{\partial y}\right)_x \left(\frac{\partial y}{\partial r}\right)_\theta\right\}_{wall} \tag{A2}$$

where

$$\left(\frac{\partial x}{\partial r}\right)_\theta = \cos\theta$$

$$\left(\frac{\partial y}{\partial r}\right)_\theta = \sin\theta$$

Expressing $\left(\frac{\partial u}{\partial x}\right)_y$ and $\left(\frac{\partial u}{\partial y}\right)_x$ in terms of the (ξ, η) coordinates one gets

$$\left(\frac{\partial u}{\partial r}\right)_{wall} = \cos\theta \left\{\left(\frac{\partial u}{\partial \xi}\right)_\eta \left(\frac{\partial \xi}{\partial x}\right)_y + \left(\frac{\partial u}{\partial \eta}\right)_\xi \left(\frac{\partial \eta}{\partial x}\right)_y\right\}_{wall} + \sin\theta \left\{\left(\frac{\partial u}{\partial \xi}\right)_\eta \left(\frac{\partial \xi}{\partial y}\right)_y + \left(\frac{\partial u}{\partial \eta}\right)_\xi \left(\frac{\partial \eta}{\partial y}\right)_x\right\}_{wall} \tag{A3}$$

Since $u = 0$ at the wall, and since the wall surfaces correspond to lines of η = constant, one has $\left(\frac{\partial u}{\partial \xi}\right)_\eta = 0$ at the wall. With this simplification, Equation (A3) becomes

$$\left(\frac{\partial u}{\partial r}\right)_{wall} = \left(\frac{\partial u}{\partial \eta}\right)_{wall} \left\{\cos\theta \left(\frac{\partial \eta}{\partial x}\right)_y + \sin\theta \left(\frac{\partial \eta}{\partial y}\right)_x\right\}_{wall} \tag{A4}$$

From Equation (3*c*) one may write

$$\left(\frac{\partial \eta}{\partial x}\right)_y = \frac{1 - \cos\xi \cosh\eta}{c} \tag{A5}$$

$$\left(\frac{\partial \eta}{\partial y}\right)_x = \frac{-\sin\xi \sinh\eta}{c} \tag{A6}$$

Combining Equations (A4), (A5), and (A6) one gets

$$\left(\frac{\partial u}{\partial r}\right)_{wall} = -\left\{\frac{(\cos\xi \cosh\eta - 1)}{c\cos\theta}\frac{\partial u}{\partial \eta}\right\}_{wall} \tag{A7}$$

A relation between ξ and θ along the wall surfaces is required and may be obtained by considering the geometry shown in Figure 1. If S is the x coordinate of the center of the circle involved, one may write

$$\tan\theta = \frac{y}{x - S} \tag{A8}$$

Substituting for x and y from Equations (3a) and (3b) into Equation (A8) and using the relations $S = S_1 = c \coth\alpha$ and $S = S_2 = c \coth\beta$ for the inner and outer circles, respectively, one obtains

$$\tan\theta)_{\substack{\text{inner}\\\text{wall}}} = \frac{\sinh\alpha \sin\xi}{\cosh\alpha \cos\xi - 1} \tag{A9}$$

$$\tan\theta)_{\substack{\text{outer}\\\text{wall}}} = \frac{\sinh\beta \sin\xi}{\cosh\beta \cos\xi - 1} \tag{A10}$$

Using the plus sign for the inner wall and the minus sign for the outer wall in Equation (A1) one gets

$$\tau_{\substack{\text{inner}\\\text{wall}}} = \tau_1 = \frac{\mu(1 - \cosh\alpha\cos\xi)}{r_1 \sinh\alpha\cos\theta} \frac{\partial u}{\partial\eta}\Big)_{\eta=\alpha} \tag{A11}$$

$$\tau_{\substack{\text{outer}\\\text{wall}}} = \tau_2 = \frac{-\mu(1 - \cosh\beta\cos\xi)}{r_2 \sinh\beta\cos\theta} \frac{\partial u}{\partial\eta}\Big)_{\eta=\beta} \tag{A12}$$

where θ and ξ along the walls are related through Equations (A9) and (A10). The average shear on each wall is given by

$$\tau_1)_{\text{avg}} = \bar{\tau}_1 = \frac{1}{\pi}\int_0^\pi \tau_1\, d\theta \tag{A13}$$

$$\tau_2)_{\text{avg}} = \bar{\tau}_2 = \frac{1}{\pi}\int_0^\pi \tau_2\, d\theta \tag{A14}$$

where the integration is performed over the range $0 \leq \theta \leq \pi$ because of symmetry about the x axis. From Equations (A11) to (A14), values of the ratio of local to average shear stress on each wall, namely $\tau_1/\bar{\tau}_1$ and $\tau_2/\bar{\tau}_2$, may be calculated.

Manuscript received May 5, 1964; revision received November 23, 1964; paper accepted November 25, 1964.

Normal Stress and Viscosity Measurements for Polymer Solutions in Steady Cone-and-Plate Shear

MICHAEL C. WILLIAMS

University of Wisconsin, Madison, Wisconsin

Normal stress and viscometric measurements were made on nine polymer solutions with cone-and-plate instruments. Temperature, concentration, molecular weight, and chemical structure were varied. Zero-shear viscosities, obtained by extrapolation of falling-sphere data, ranged from 0.7 to 380 poise.

A brief description is given of a normal stress-measurement apparatus, incorporating fast-response strain gauge pressure transducers. Measurements were made at shear rates between 5 and 2,800 sec.$^{-1}$, sometimes necessitating a considerable correction for inertial forces.

Non-Newtonian viscosity, normal stress, recoverable shear strain, and elastic modulus are presented in terms of modified Ferry reduced variables.

When viscoelastic liquids are subjected to shear, they exhibit a number of unique phenomena which distinguish them from so-called *Newtonian fluids*. Even in the restrictive case of steady viscometric flows studied here, their elastic properties give rise to non-Newtonian viscosity and various normal stress effects. In polymer solutions, such behavior is thought to be a consequence of cooperative configurational changes within and between solute molecules. These phenomena are currently the subject of considerable experimental investigation for the purposes of guiding engineering design, revealing the mechanical implications of fluid structure, and evaluating the many constitutive (rheological) equations which have been proposed.

The work reported here involved measurement of non-Newtonian viscosity and one normal stress function with cone-and-plate instruments. Supplementary information was obtained by falling-sphere viscosity tests.

CONE-AND-PLATE THEORY

Consider the geometry of Figure 1, in which a cone of radius R is rotating steadily with angular velocity Ω about an axis perpendicular to a stationary plate, and the cone vertex makes point contact with the plate. An incompressible fluid contained between the two surfaces is commonly assumed (5, 22) to flow in accordance with

Michael C. Williams is at the Institute of Theoretical Science, University of Oregon, Eugene, Oregon.